2022 - Nonlinear Session

Direct numerical simulation of acoustic turbulence: Zakharov-Sagdeev spectrum

Evgeny Kochurin[1,2], E.A. Kuznetsov[1,3,4]

[1]Skolkovo Institute of Science and Technology, Moscow, Russia
[2]Institute of Electrophysics, Ural Division of RAS, Ekaterinburg, Russia
[3]Lebedev Physical Institute, RAS, Moscow, Russia
[4]Landau Institute for Theoretical Physics, RAS, Chernogolovka, Moscow region, Russia
E-mail:kochurin@iep.uran.ru

19 December, 2022

Weak turbulence theory (Kolmogorov-Zakharov's spectrum)

Wave turbulence occurs when nonlinear waves interact with each other. This phenomenon is ubiquitous: oceanographic waves, plasma waves in the solar wind, nonlinear optical waves, elastic waves, or gravitational waves. A weakly nonlinear theory (or weak turbulence theory) predicts analytically the wave spectra in various domains involving nonlinear waves. Such Kolmogorov-Zakharov's (KZ) spectra can be also obtained by dimensional analysis, [Nazarenko et al. (2003)].

The Zakharov-Filonenko spectrum (1967) for isotropic capillary wave turbulence is the example of KZ-spectrum:

$$S(\mathbf{k}) = < |\eta_{\mathbf{k}}|^2 > = C(\sigma/\rho)^{-3/4} P^{1/2} k^{-(19/4)},$$

where C is a constant, σ is the surface tension coefficient, ρ is the mass density of a liquid, P is the energy dissipation rate.

Capillary turbulence of a free surface / A picture from the internet

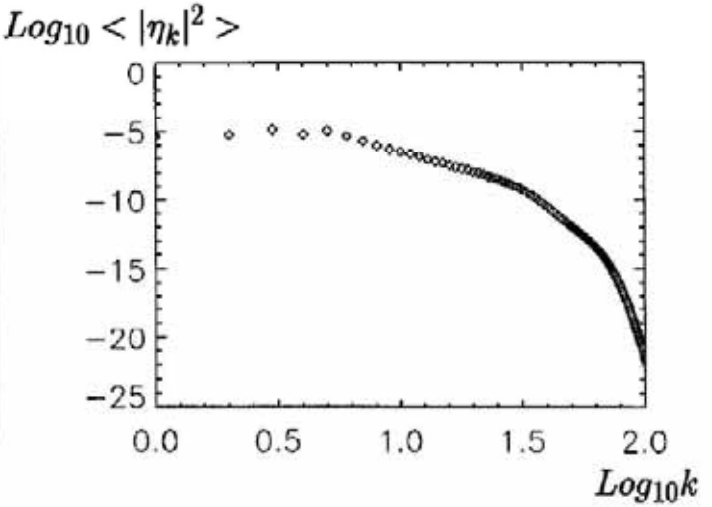

A. N. Pushkarev, V. E. Zakharov / Phys. Rev. Lett. (1996)

Kolmogorov-Zakharov's spectrum for acoustic wave turbulence

The dispersion relation for non-dispersive wave system (acoustic waves) reads

$$\omega \simeq ck, \qquad c \quad \text{is the sound speed.}$$

The weak turbulence theory of acoustic turbulence is proposed in [V. E. Zakharov, R. Z. Sagdeev, (1970)]. The Zakharov-Sagdeev spectrum has the following form:

$$E_k = c^{1/2} P^{1/2} k^{-3/2}, \qquad n_{\mathbf{k}} = c^{-1/2} P^{1/2} k^{-9/2}. \tag{1}$$

The energy density of acoustic wave field E_k is related with wave action n_k as $E_k = 4\pi c k^3 n_k$. The spectrum (1) is the exact analytical solution of the kinetic equation:

$$\frac{\partial E_k}{\partial t} + \frac{\partial P_k}{\partial k} = 0,$$

$$P_k = -16\pi^3 \int k' dk' \int |V_{k_1 k_2 k_3}|^2 f(k, k_1, k_2) k'^2 k_1^2 k_2^2 (n_{k_1} n_{k_2} + n_{k'} n_{k_2} - n_{k'} n_{k_1}) \delta_{k_2 - k_1 - k} d\mathbf{k}_1 d\mathbf{k}_2,$$

with with the interaction matrix $V_{k_1 k_2 k_3}$

$$V_{k_1 k_2 k_3} \approx (|\mathbf{k}||\mathbf{k}_1||\mathbf{k}_2|)^{1/2}.$$

The Zakharov-Sagdeev spectrum (1) is well known. It has been numerically confirmed only within the framework of the kinetic equations, [Zakharov, Musher, (1973)]. The spectrum (1) has not yet been reproduced within the framework of direct numerical simulation (DNS) methods.

Kadomtsev-Petviashvili's spectrum for acoustic wave turbulence

Another approach to describe the acoustic wave turbulence is proposed by [Kadomtsev and Petviashvili, Doklady USSR, (1973), Kuznetsov JETP Lett. (2004)]. Accordingly to KP spectrum, the acoustic turbulence is an ensemble of acoustic shock waves. The energy density is discontinuous at the shock wave front. Thus, the KP spectrum is

$$E_\omega \sim \omega^{-2}, \qquad E_k \sim\sim k^{-2}.$$

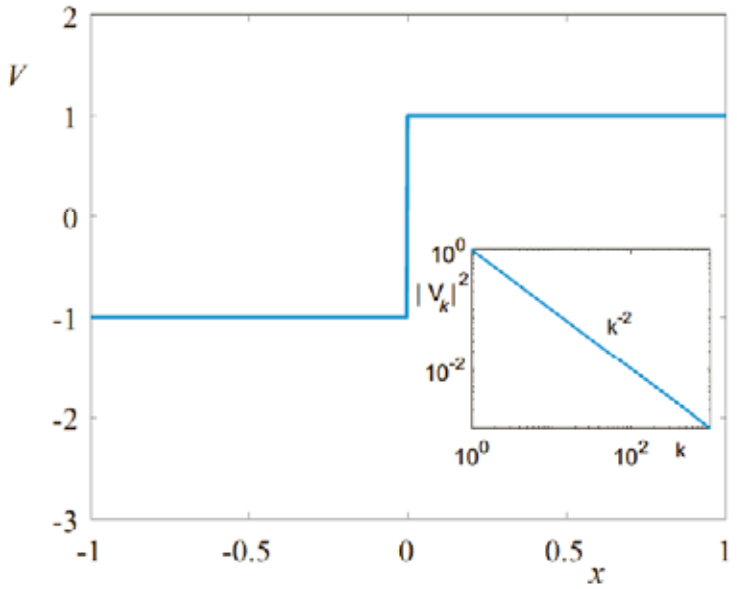

Acoustic turbulence of second sound waves in He II

It is known that acoustic turbulence can develop in He II [G.V. Kolmakov, et. al. Phys. Rev. Lett. (2006)]. The experimental and numerical research results of [G.V. Kolmakov, et. al. Phys. Rev. Lett. (2006)] are shown in the figure below. The author's result indicate the formation KP spectrum.

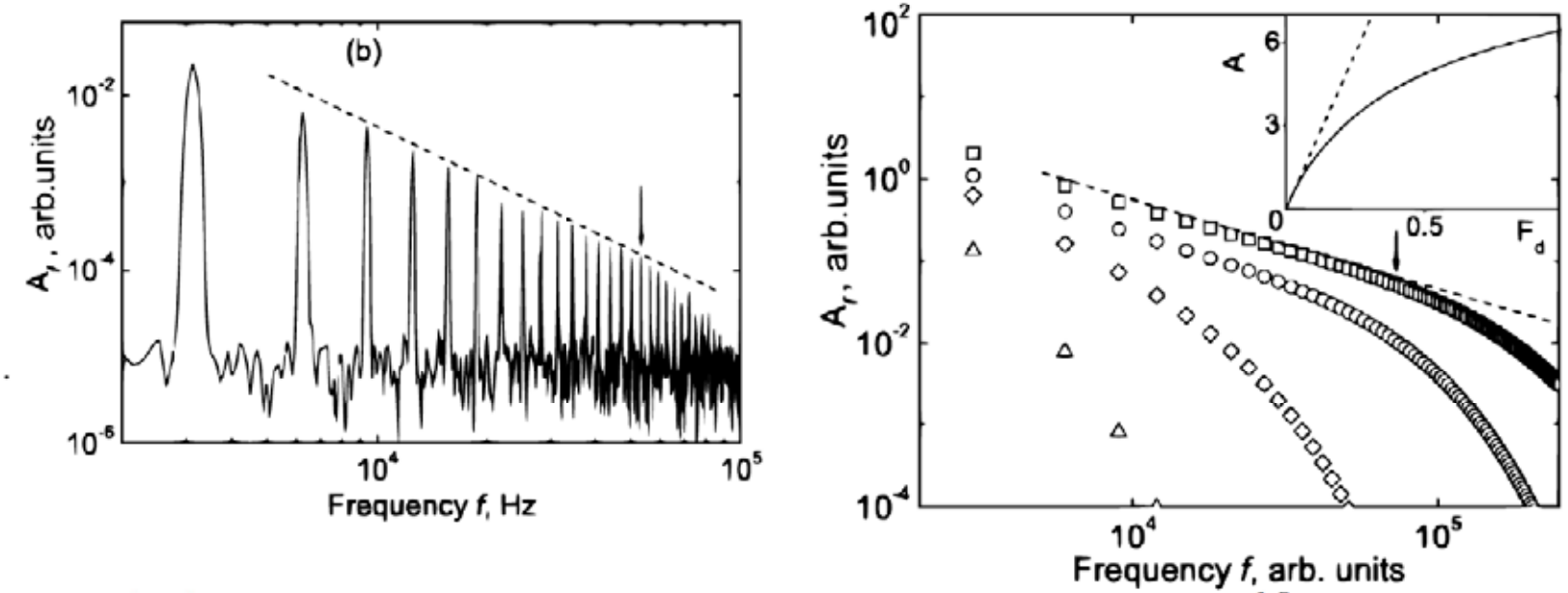

Рис. 1: (left) Experimental power spectral amplitudes, dashed line corresponds to $f^{-1.5}$, (right) numerical simulation results based model ODE system, dashed line corresponds to f^{-1}. See details in [G.V. Kolmakov, et. al. Phys. Rev. Lett. (2006)].

The model equation for weakly dispersive wave turbulence

We consider a three-dimensional wave field described by a scalar function of coordinates $u(x, y, z)$. The model equation for $u(x, y, z)$ is proposed in [Zakharov, J. Appl. Mech. Tech. Phys. (1965)]

$$u_{tt} = \Delta u - 2a^2 \Delta\Delta u + \Delta u^2 - \gamma_k u_t, \tag{2}$$

where a is the dispersion length, Δ is the Laplace operator, γ_k is the viscosity operator acting at small scales. The dispersion relation is

$$\omega_k^2 = k^2 + 2a^2 k^4,$$

The normal variables a_k and a_k^* for the equation (2) are introduced as

$$u_k = -\frac{ik}{2\omega_k^{1/2}}(a_k - a_k^*), \qquad \dot{u}_k = \frac{k\omega_k^{1/2}}{2}(a_k + a_k^*).$$

The interaction matrix [Zakharov, (1965)] has the form:

$$V_{k_1 k_2 k_3} \approx \frac{1}{\sqrt{8}} \left(\frac{\mathbf{k}^2 \mathbf{k}_1^2 \mathbf{k}_2^2}{\omega \omega_1 \omega_2} \right)^{1/2}.$$

which coincides with acoustic type interaction coefficients in the limit $a \to 0$. The Kolmogorov-Zakahrov spectrum is applicable in this limit:

$$n_k = |a_k|^2 = C_{KZ} k^{-9/2}, \qquad \Rightarrow \qquad |u_k|^2 = C_{KZ} k^{-7/2},$$

where C_{KZ} is the Kolmogorov-Zakharov constant.

The model equation for weakly dispersive wave turbulence

The governing equation refers to Hamiltonian systems, it can be represented as a system of two equations:

$$u_t = \frac{\delta H}{\delta \phi}, \qquad \phi_t = -\frac{\delta H}{\delta u}, \tag{3}$$

where ϕ has the meaning of the hydrodynamic potential, and the Hamiltonian H is written as

$$H = \frac{1}{2}\int \left[(\nabla\phi)^2 + u^2\right] d\mathbf{r} + \int a^2(\nabla u)^2 d\mathbf{r} + \frac{1}{3}\int u^3 d\mathbf{r} \equiv$$

$$\equiv H_1 + H_2 + H_3. \tag{4}$$

The Hamiltonian (4) has three terms. The first H_1 is the sum of the kinetic and potential energies of linear dispersionless waves. The second term H_2 is responsible for the dispersive part of the wave energy, and H_3 describes the nonlinear interaction of waves.

With account of both pumping and damping terms, the equations (3) are written in the form:

$$u_t = -\Delta\phi + \mathcal{F}(\mathbf{k}, t) - \gamma_k u, \tag{5}$$

$$\phi_t = -u + 2a^2\Delta u - u^2, \tag{6}$$

where the operator γ_k responsible for dissipation and the forcing term $\mathcal{F}(\mathbf{k}, t)$.

Numerical scheme and parameters

With account of both pumping and damping terms, the equations (3) are written in the form:

$$u_t = -\Delta\phi + \mathcal{F}(\mathbf{k}, t) - \gamma_k u, \tag{7}$$

$$\phi_t = -u + 2a^2\Delta u - u^2, \tag{8}$$

where the operator γ_k responsible for dissipation and the forcing term $\mathcal{F}(\mathbf{k}, t)$ are given in Fourier space as:

$$\begin{aligned}
\gamma_k &= 0, \quad k \le k_d, \\
\gamma_k &= \gamma_0, \quad k > k_d, \\
\mathcal{F}(\mathbf{k}, t) &= F(k) \cdot \exp[iR(\mathbf{k}, t)], \\
F(k) &= F_0 \cdot \exp[-(k - k_1)^4 / k_2^4], \quad k \le k_2, \\
F(k) &= 0, \quad k > k_2.
\end{aligned}$$

Here $R(\mathbf{k},t)$ are random numbers uniformly distributed in the interval $[0, 2\pi]$, γ_0 and F_0 are constants.

Time integration was performed using explicit scheme by means of the Runge-Kutta method of the fourth order accuracy with step $\delta t = 2.5 \cdot 10^{-3}$. The equations were integrated over spatial coordinates using spectral methods with the total number of harmonics $N^3 = 512^3$. Below we present results of numerical simulation for the following parameters: $k_d = 125$, $k_1 = 3$, $k_2^4 = 6$, $\gamma_0 = 100$, $a = 2.5 \cdot 10^{-3}$, $F_0 = 5 \cdot 10^5$. With this choice of parameters, the inertial interval was more than one decade. The maximum dispersion addition at the end of the inertial interval, $k = k_d$, was $(k_d a)^2 \approx 0.1$.

The algorithm is parallelized on GPU using NVidia CUDA platform. The total workspace requires near 20 Gb of video memory. The calculations were carried out on NVidia RTX 3090 with 24 Gb VRAM.

Figure 1 shows how the total energy of the system (4) evolves. The inset to Fig. 2 shows the time dependencies of the dispersive part of the energy H_2 and the nonlinear interaction energy H_3. Both contributions H_2 and H_3 turn out to be small compared to the total energy of the system (respectively, H_1).

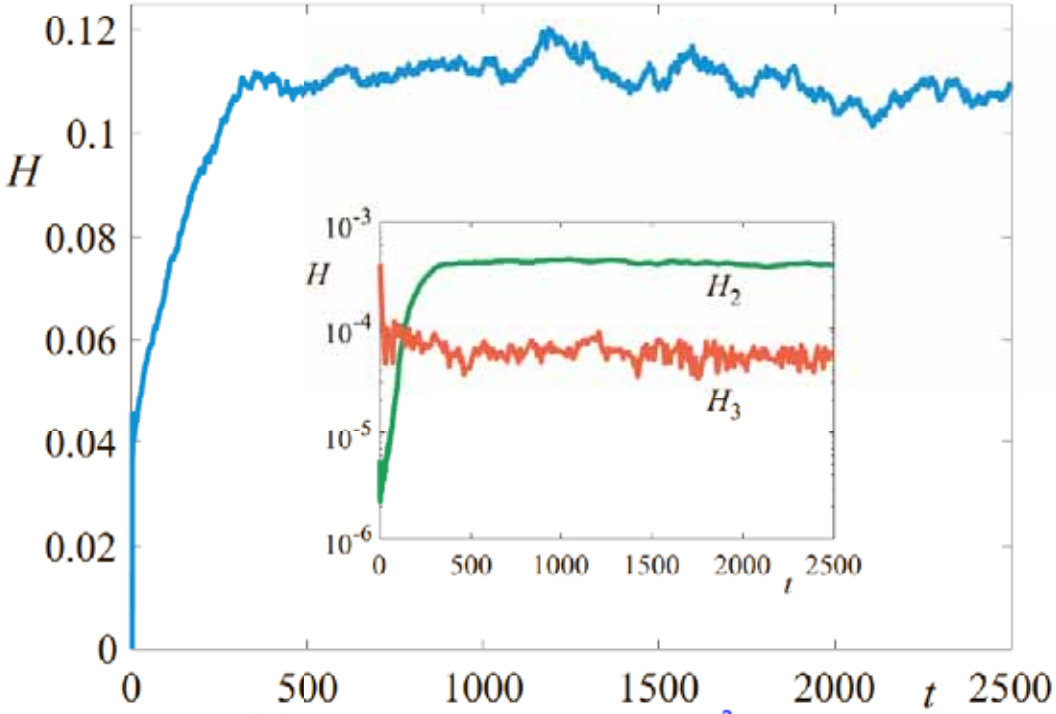

Рис. 2: Total energy of the system (4) versus time for $a = 2.5 \cdot 10^{-3}$. The inset shows the time dependencies of the dispersive part of the energy H_2 and the nonlinear interaction energy H_3.

The behavior of the spectrum of space-time Fourier transform of the function $u(\mathbf{r}, t)$ shown in Fig. 3 also testifies to the weakly nonlinear character of wave propagation.

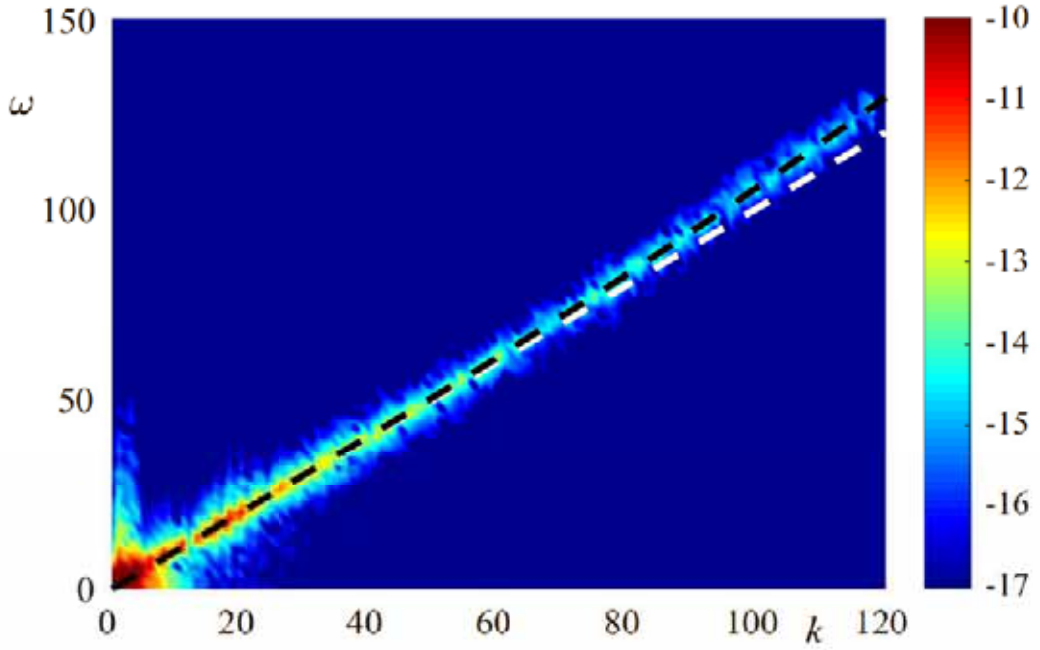

Рис. 3: The space-time Fourier transform $|u(\mathbf{k}, \omega)|^2$ is shown in logarithmic scale. The black dotted line corresponds to the exact value of the dispersion curve (??), the white dotted line corresponds to the non-dispersive wave propagation, $\omega = |\mathbf{k}|$.

Numerical simulation results

The numerical experiment shows that after the system enters the quasi-stationary state, the behavior of $u(\mathbf{r})$ acquires a complex (turbulent) character. In Fig. 4 this behavior demonstrates the dependence of the function $u(\mathbf{r})$ in the $z = 0$ plane for the quasi-stationary state at the moment $t = 2500$.

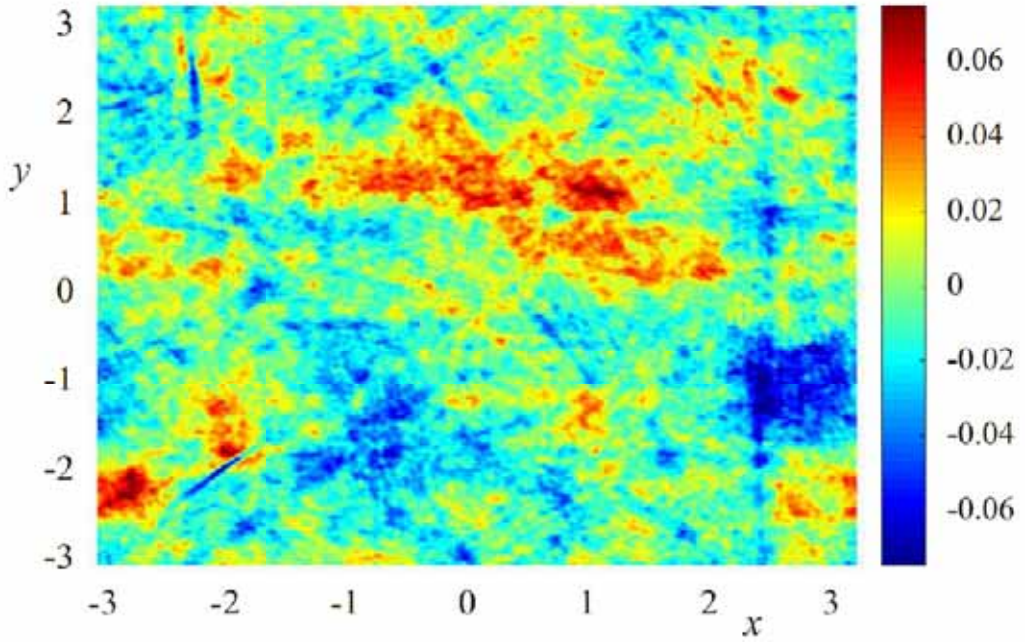

Рис. 4: Section of the function $u(\mathbf{r})$ by $z = 0$ plane is shown at the moment $t = 2500$ corresponding to the quasi-stationary state..

Numerical simulation results

On fig. 5 we present three isosurfaces of the function $|u_{\mathbf{k}}|\,(=\epsilon_k^{1/2})$. As seen, in the region of small wavenumbers, structures with a large number of jets in the form of narrow cones appear in the distribution of turbulent fluctuations. The onset of such structures is the result of resonant wave interactions at very small k close to the pumping region when dispersion can be neglected. As k increases, the cones broaden and the distribution tends to be isotropic one.

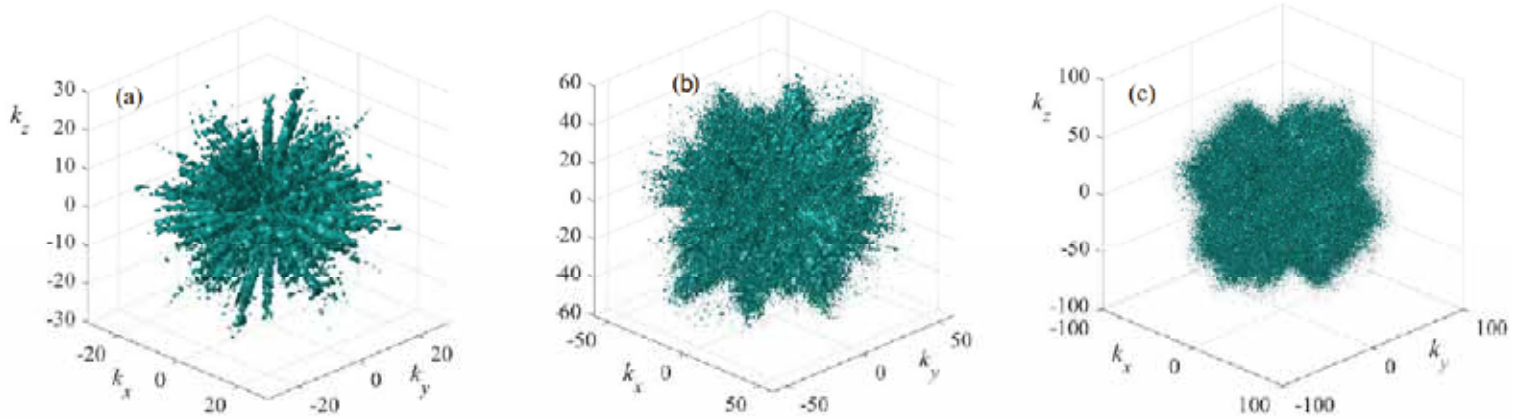

Рис. 5: Isosurfaces of the Fourier spectrum of $|u_{\mathbf{k}}| = u_0$, (a), (b) and (c) correspond to the values $u_0 = 5{\cdot}10^{-5}$, $0.5 \cdot 10^{-5}$ and $0.25 \cdot 10^{-5}$, respectively, $t = 2500$.

Numerical simulation results

The birth of jets is associated with two possible causes: linear and non-linear. The first one is the discreteness of the wave vector lattice in the pumping region, $1 \leq k \leq 6$, which inevitably leads to a small anisotropy in the excitation and differences in the growth of perturbations at the initial stage.

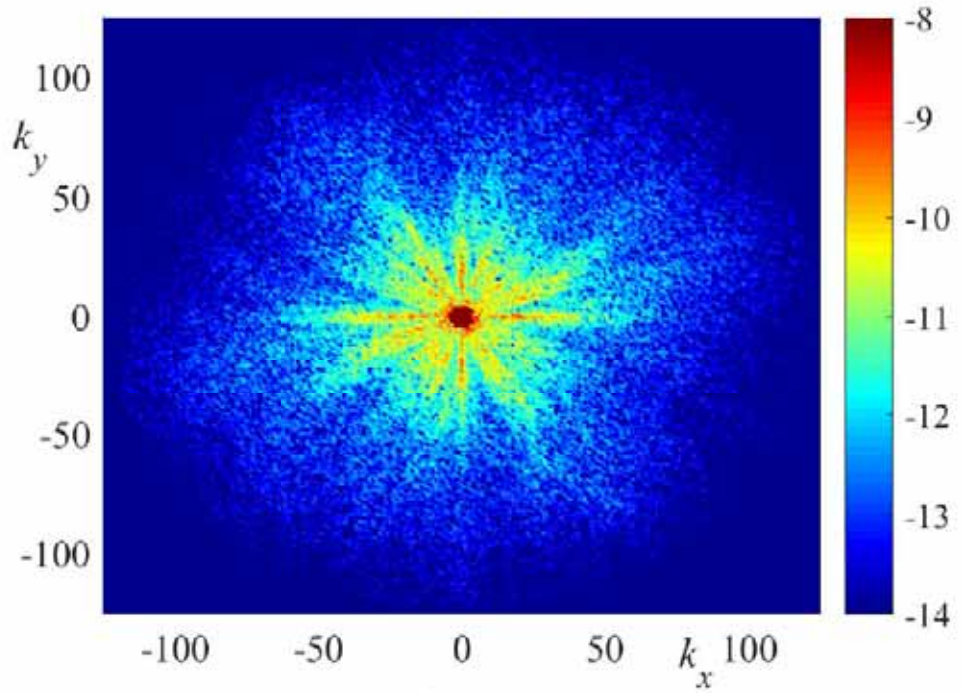

Рис. 6: Fourier spectrum of $|u_{\mathbf{k}}| \equiv \epsilon_k^{1/2}$ in section $k_z = 0$ (logarithmic scale), $t = 2500$.

Numerical simulation results

To find the turbulence spectrum $E(k)$, as noted above, it is necessary to integrate the expression $k^2\epsilon_k$ over the entire solid angle. Figure 7 shows the result of this averaging over the angle for the moment of time corresponding to the quasi-stationary state. It is clearly seen from Fig. 7 that in the regime of quasi-stationary chaotic motion, the spectrum of $E(k)$ acquires a power law behavior.

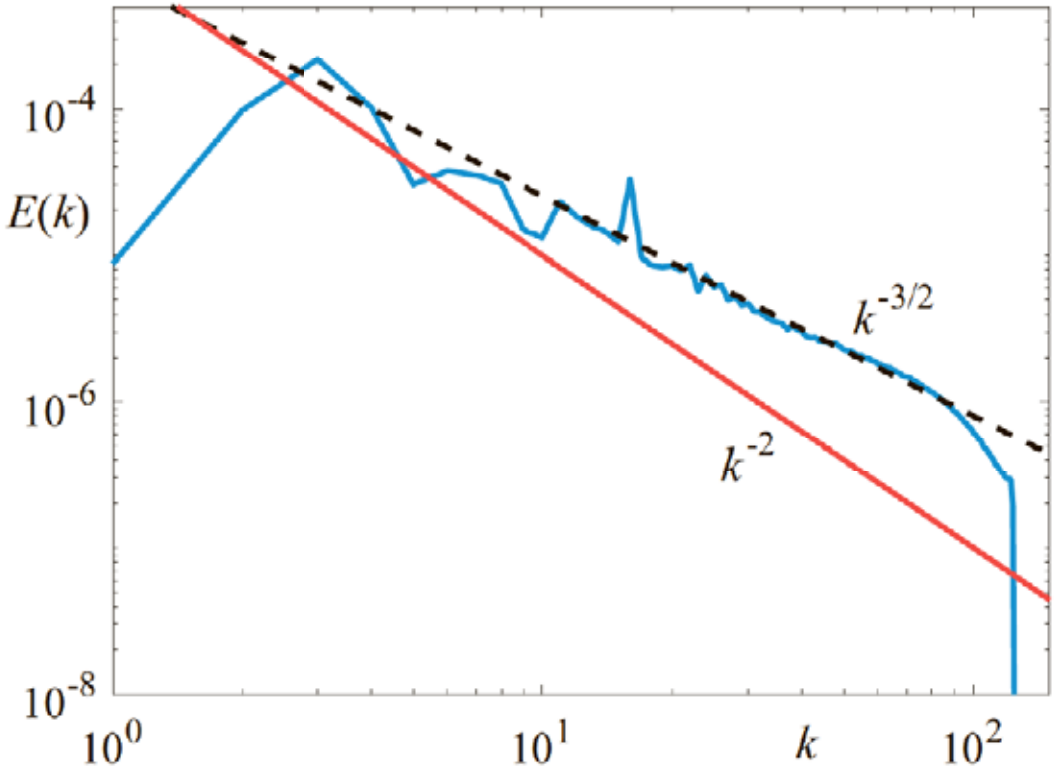

Рис. 7: The turbulence spectrum $E(k)$ measured in the quasi-stationary state, the black dotted line corresponds to the Zakharov-Sagdeev spectrum (1), the red solid line corresponds to the Kadomtsev-Petviashvili spectrum.

Previous simulation results

It should be noted that similar direct numerical simulations were carried out for quantum turbulence within the three-dimensional Gross-Pitaevskii equation. [D. Proment, S. Nazarenko, M. Onorato, Physica D (2012)].

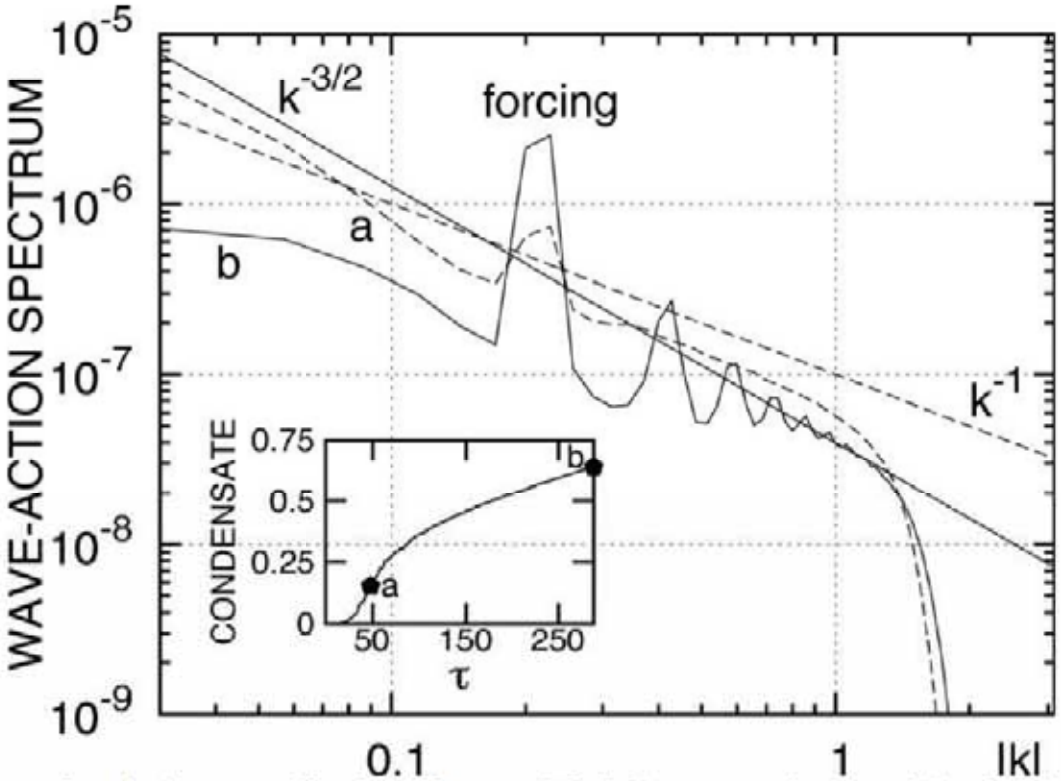

Рис. 8: The spectra of turbulence oscillations for non-ideal Bose gas simulated in the framework of Gross-Pitaevskii equation.

Conclusions

In the present work, direct numerical simulation of three-dimensional acoustic turbulence in a medium with weak positive dispersion is carried out, taking into account the pumping and dissipation of energy. It was established in the work that the system of nonlinear interacting weakly dispersive waves quickly enough passes into the quasi-stationary chaotic state, which is a developed wave turbulence. In the quasi-stationary regime, the wave field acquires a complex, chaotic character. In the long-wavelength region, close to pumping, we observed in the turbulence spectrum the appearance of narrow jets in the form of cones, which expand upon transition to the short-wave region. The latter leads to the fact that the spectral energy density ϵ_k tends in the region of large k to an isotropic distribution, for which the dispersion remains weak. In this range of scales, the turbulence spectrum calculated in the stationary state agrees with a high accuracy with the analytical Zakharov-Sagdeev's spectrum of weak acoustic turbulence.

The authors thank V.E. Zakharov for helpful discussions. This work was financially supported by the Russian Science Foundation (grant no. 19-72-30028).

E.A. Kochurin, E.A. Kuznetsov, Direct numerical simulation of acoustic turbulence: Zakharov-Sagdeev spectrum, JETP Letters, 12, (2022)

Thank you for your attention!

Numerical simulation results: non-dispersive case $a = 0$

Figure 1 shows how the total energy of the system (4) evolves.

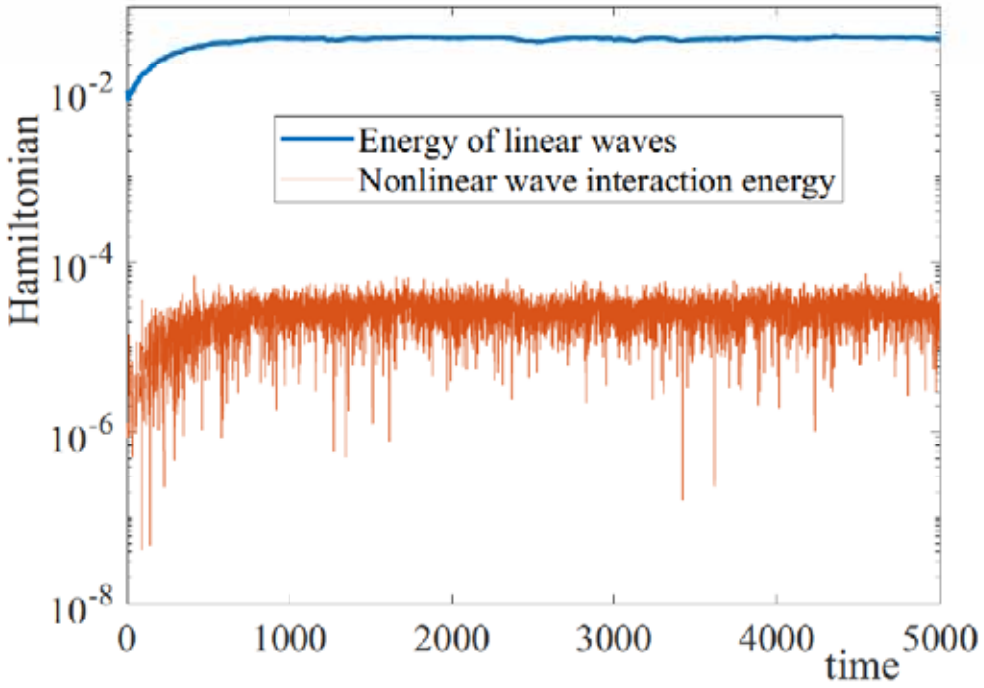

Рис. 9: Total energy of the system (4) versus time for $a = 0$.

Numerical simulation results: non-dispersive case $a = 0$

We present three isosurfaces of the function $|u_{\mathbf{k}}| (= \epsilon_k^{1/2})$. As seen, in the region of small wavenumbers, structures with a large number of jets in the form of narrow cones appear in the distribution of turbulent fluctuations. The onset of such structures is the result of resonant wave interactions at very small k close to the pumping region when dispersion can be neglected. As k increases, the cones broaden and the distribution tends to be isotropic one.

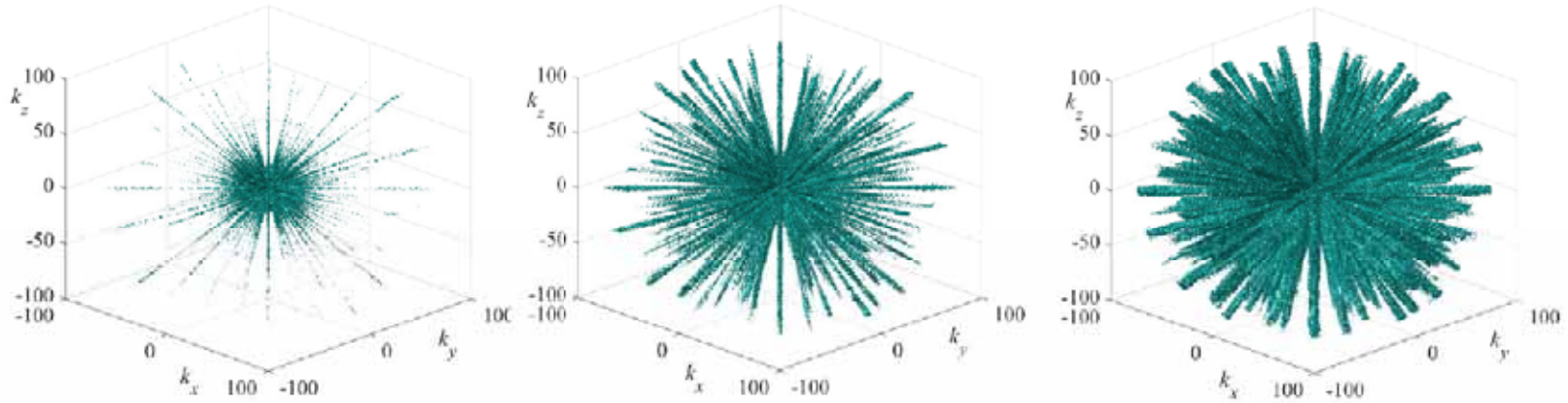

Рис. 10: Isosurfaces of the Fourier spectrum of $|u_{\mathbf{k}}| = u_0$, (a), (b) and (c) correspond to the values $u_0 = 5 \cdot 10^{-5}$, $0.5 \cdot 10^{-5}$ and $0.25 \cdot 10^{-5}$, respectively, $t = 2500$.

Numerical simulation results: non-dispersive case $a = 0$

The birth of jets is associated with two possible causes: linear and non-linear. The first one is the discreteness of the wave vector lattice in the pumping region, $1 \leq k \leq 6$, which inevitably leads to a small anisotropy in the excitation and differences in the growth of perturbations at the initial stage.

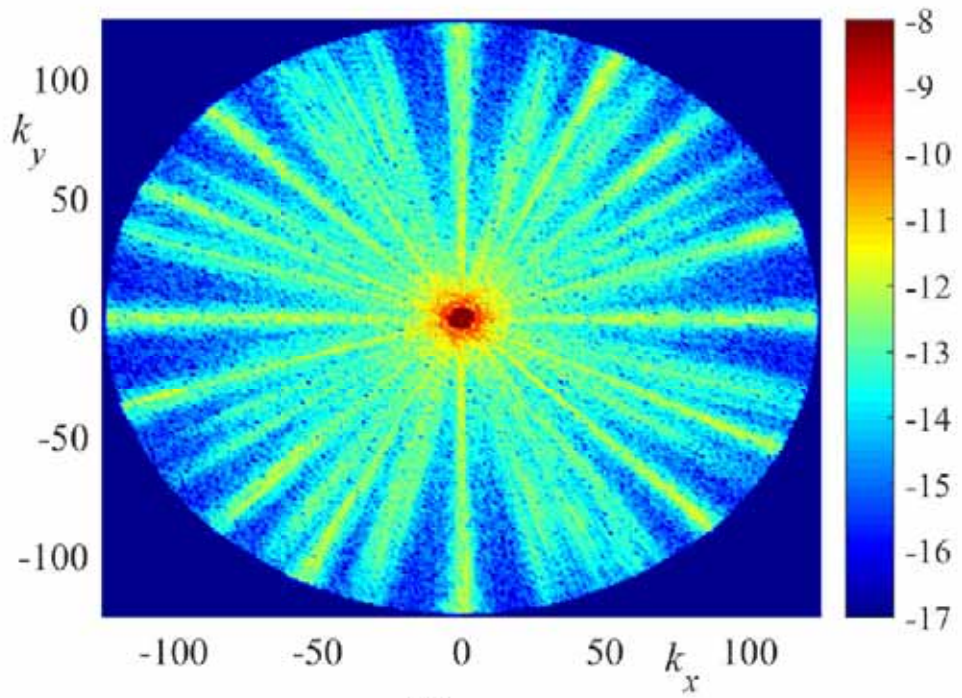

Рис. 11: Fourier spectrum of $|u_{\mathbf{k}}| \equiv \epsilon_k^{1/2}$ in section $k_z = 0$ (logarithmic scale), $t = 2500$.

Numerical simulation results: non-dispersive case $a = 0$

The numerical experiment shows that after the system enters the quasi-stationary state, the behavior of $u(\mathbf{r})$ acquires a complex (turbulent) character. In Fig. 4 this behavior demonstrates the dependence of the function $u(\mathbf{r})$ in the $z = 0$ plane for the quasi-stationary state at the moment $t = 2500$.

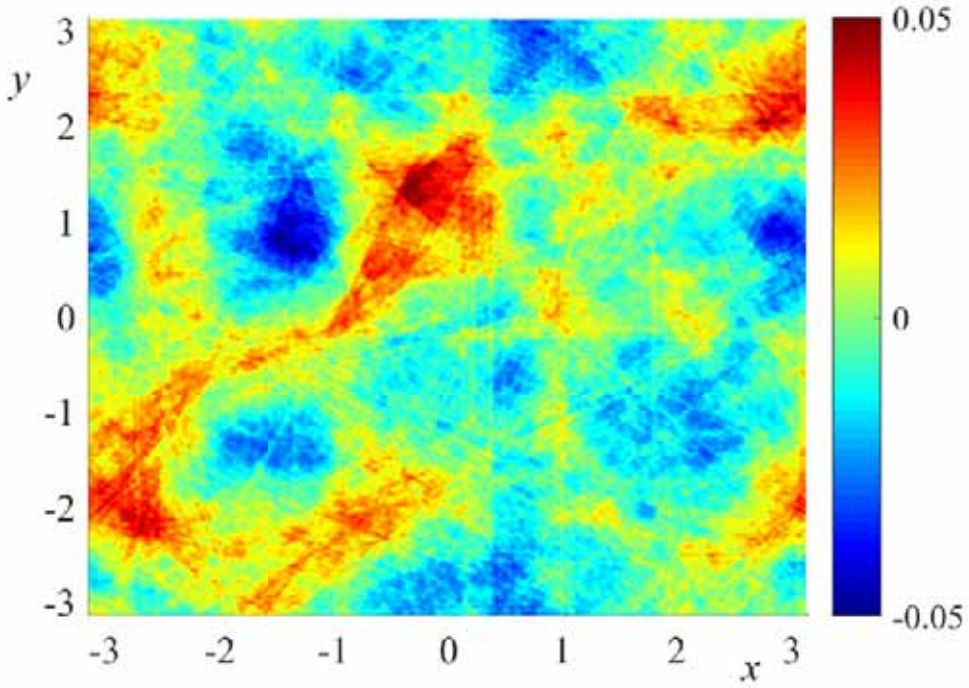

Рис. 12: Section of the function $u(\mathbf{r})$ by $z = 0$ plane is shown at the moment $t = 2500$ corresponding to the quasi-stationary state, $a = 0$.

Numerical simulation results: non-dispersive case $a = 0$

The energy turbulence spectrum for pure non-dispersive case is presented in the Figure. The grey line corresponds to non-averaged spectrum over integer k. We can see large deviations from power-law dependency. Apparently, it is necessary to average the spatial spectrum with respect to a small solid angle inside the formed cones.

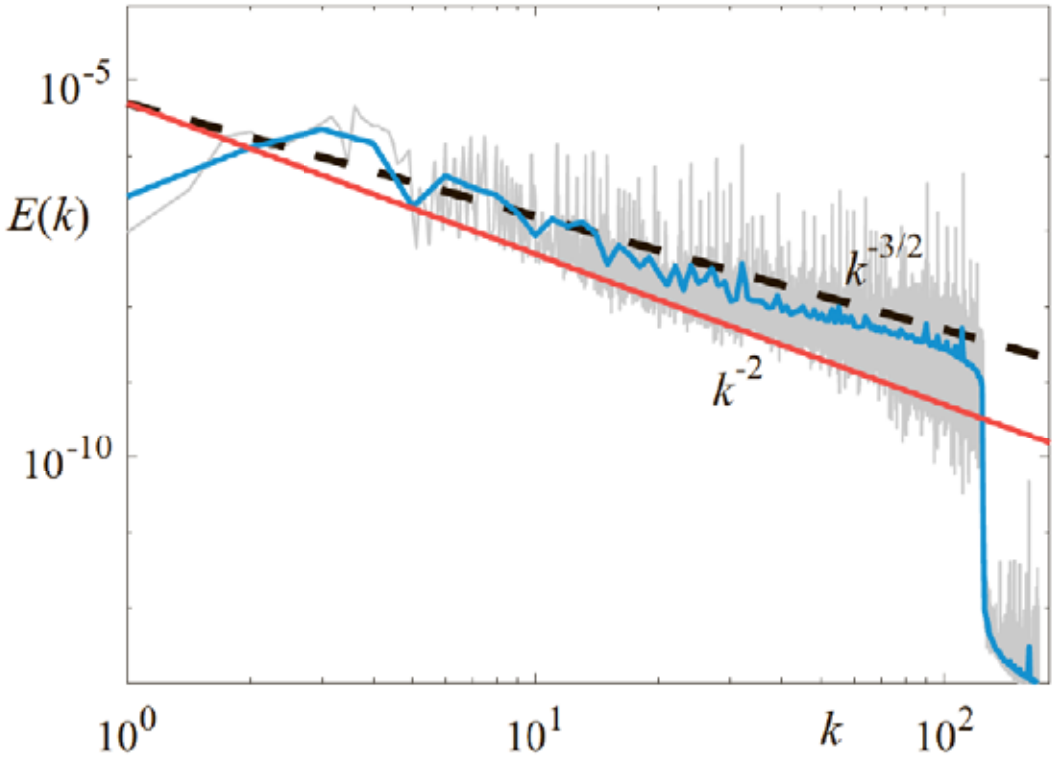

Рис. 13: The turbulence spectrum $E(k)$ measured in the quasi-stationary state, the black dotted line corresponds to the Zakharov-Sagdeev spectrum (1), the red solid line corresponds to the Kadomtsev-Petviashvili spectrum.